8 Verification of models for tensile strength of paper

8.1 Introduction

An important aspect of modelling tensile strength is to fully verify the model with experimental data. Verification of a model is at least equally important as the development of the model. It is well known that fully verifying models for tensile strength is usually very difficult because it requires a wide range of data and some parameters, as discussed in Chapter 2, are difficult or extremely difficult to measure in practice. A wide range of paper and fibre properties have been measured in this project.

A very important part of this project has been to develop new techniques for measuring the difficult parameters so as to obtain a full range of data for fully testing the important models developed in previous studies and the new model developed in this project. In this project we have developed new techniques to measure some of these difficult parameters including fibre dimensions in a sheet and the number of fibre-fibre contacts in paper. These techniques have been presented in Chapter 4. The experimental data measured by these new techniques have been discussed in Chapters 6 and 7. Cutting wet handsheets and hydrocyclone fractionation were employed to vary only fibre length and fibre cross sectional properties, respectively. These experiments have been discussed in Chapter 5. For the first time, such comprehensive sets of data are available for testing models of paper tensile strength.

In this Chapter, we will first test the Page equation, which is the most commonly used model for tensile strength, by using experimental data obtained in this project. The key parameter in the simple fracture model, r, is the ratio of peak load in a fibre to the average load in the fibre (see Chapter 3). This is first calculated by using the shear lag model. Several types of shear lag models will be examined for this purpose. This will be followed by discussion of a newly developed direct stress transfer theory. The stress distribution in a fibre is simulated based on the new theory. The peak average load in the fibre is used to calculate the tensile strength and compared with the measured tensile strength of paper.

8.2 Verification of the Page equation

As discussed in Chapter 2, the Page equation (as given in Equation 8.1) is the most commonly used model for the tensile strength of paper. However, this equation has never been fully verified with experimental data.

$$\frac{1}{T} = \frac{9}{8Z} + \frac{12A\rho g}{bPL(RBA)} \qquad \textbf{8. 1}$$

In Equation 8.1, T is the tensile strength (km), Z is the zero span breaking length (km), A is the average fibre cross sectional area (m^2), ρ is the density of the fibre (g/m^3), g is the acceleration due to gravity (m/s^2), P is the perimeter of the fibre cross section (m), L is the length of the fibre (m) and RBA is the relative bonded area

In the work in this thesis, all of the parameters in Equation 8.1 except the fibre-fibre bond strength and the fibre wall density have been measured. The fibre wall density was assumed to be $\rho = 1500 kg/m^3$. According to Page (Page 1969) the length weighted fibre length should be used for this calculation. The perimeter was calculated by $2(D_w + D_h)$. The fibre-fibre bond strength was used as a fitting parameter. The calculated tensile strength by Equation 8.1 was then fit to the measured tensile strength using a least squares method. The data of two series of samples were used for the fits. One series of samples was made from fibres with different fibre length, which was changed by wet cutting the fibres with a die (refer to subsection 5.2.3). The other series of samples was made from fibres with different cross-sectional dimensions, which was altered by hydrocyclone fractionation (the accepts and rejects see subsection 5.2.2). For each set of sheets, the density and strength were altered by wet pressing at different pressing pressures. The details about the pressing pressures used and the sheet preparation techniques are described in subsection 5.2.1).

It was found that the bond strength for the best fit for the cut fibres is 3.0×10^6 N/m^2, compared to 2.0×10^6 N/m^2 for the accepts and 1.9×10^6 N/m^2 for the rejects. These values of bond strength are of the same order of the previous measurements in the literature. Mayhood, Kallmes and Cauley (Mayhood 1962) reported that the bond strength of 2.9×10^6 N/m^2 for spruce sulfite fibres and 3.6×10^6 N/m^2 for spruce sulfate

fibres. In the work here, the fitted values for the rejects (mainly summer wood fibres) and the accepts (mainly springwood fibres) bond strengths show about the same value. This conflicts with previous measurements by McIntosh (McIntosh 1962) who measured the bond strength between fibre and shive as 2.7×10^6 N/m^2 for springwood fibres and 7.1×10^6 N/m^2 for the summerwood fibres.

It is also difficult to explain why the bond strengths of the rejects and accepts are lower than the whole pulp. One possible reason why the bond strength might be lower is that both accepts and rejects were screened to thicken the stock after fractionation. This will have the effect of removing some of the fines from the stock. However, the effect of the removal of the fines on the bond strength is likely to be minimal. This is because the samples were unrefined and so it was likely that fine material made up only a small fraction of the total stock. Certainly it is hard to see how the removal of these fines in the accepts and rejects could reduce the shear bond strength by 50%.

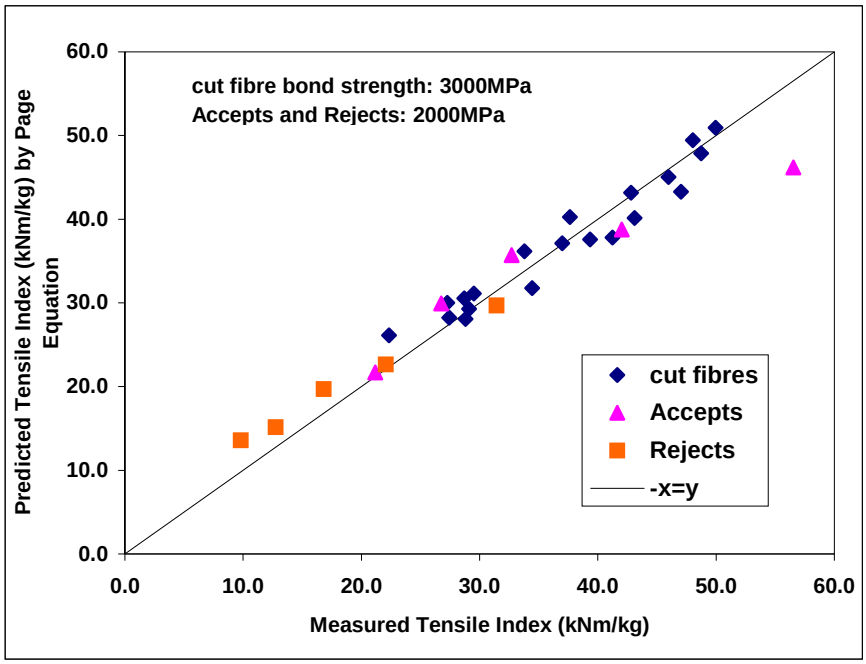

Figure 8-1 Correlation between the measured and predicted tensile strength by Page equation using different shear bond strengths

Figure 8-1 shows the correlation between the measured tensile strength and the predicted tensile strength by the Page equation when the bond strength was set to be 3.0×10^6 N/m^2 for the cut fibres and 2.0×10^6 N/m^2 for the fractionated fibres. It shows a very good correlation between the measurements and the predictions. If a single bond

strength was used in the fit between the measurements and the predictions, the best fit bond strength for all of the samples was 2.6×10^6 N/m^2 and the correlation between the measurements and the predictions is much poorer as shown in Figure 8-2.

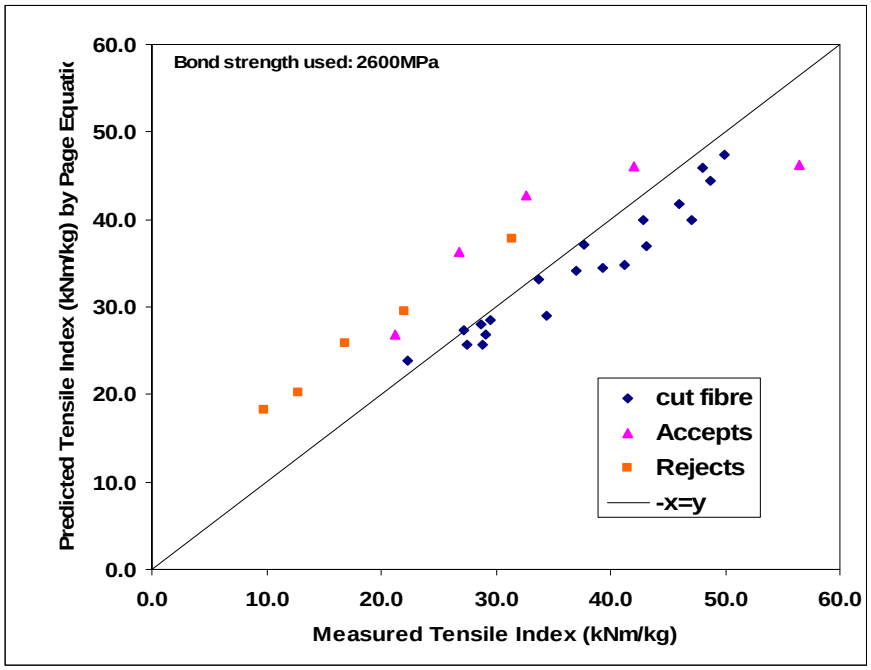

Figure 8-2 Correlation between the measured and predicted tensile strength by Page equation using same shear bond strength

In deriving the equation, Page assumed that all fibre-fibre bonds act cooperatively along the length of a fibre and the fibre-fibre bond strength, β, is given by:

$$\beta = bP(RBA)l_f / 4 \qquad \textbf{8. 2}$$

where b is shear bond strength per unit bonded area, and the other parameters are the same as in Equation 8.1.

The calculation seems to consider that all types of fibres would bond in the same manner if they have the same length and perimeter. This might be reasonable for one type of fibre but not necessarily correct for different types of fibres. This equation also assumes that the bonds act co-operatively. That is the contribution of the bonds is the same whether they are at the end of the fibre or in the middle. This assumption also contradicts the shear lag model, which assumes that the bonds at the end of the fibre are the most heavily loaded.

Thus it seems from our data that the Page equation can provide a reasonable prediction for paper strength only if the bond strength is used as a fitting parameter for each set of data. The explanation for this is that the Page equation is probably not correctly accounting for the effect that changes in fibre morphology has on paper strength. Given that all the fibre morphology variables appear together with the fibre-fibre bonding in the right hand term in the Page equation, then any inadequacies in the way that the Page equation takes fibre morphology effects into account can be compensated for by adjusting the bond strength.

The above discussion suggests that the Page equation gives only a reasonable qualitative description of how trends in fibre and sheet properties will affect paper strength and that it cannot be relied upon for quantitative predictions. Thus the need for a quantitative model for paper strength remains.

8.3 Examination of Fibre Fracture Model

The fracture of paper can be triggered either by the fracture of fibre or the failure of fibre-fibre bonds. As reviewed in Chapter 2, it is still not quite clear what triggers the fracture of a sheet of paper. The first premise of Page equation proposes that fibre fracture initiates the fracture of the paper. The tests of the Page equation have shown that this premise is acceptable. In this project we also believe that the fracture of paper is triggered by the fracture of fibres that are aligned with the applied stress. A simple fibre fracture model has been developed as discussed in Chapter 3. This model is written as:

$$T = \frac{1}{r}\frac{8}{9}Z \qquad \textbf{8. 3}$$

where T is tensile index, Z is zero span tensile index and r is a constant for a given paper

To test the fibre fracture model (Equation 8.3), we need first to determine the value of r in the equation. The key variable, r, in Equation 8.3 is defined as the ratio of peak load to the average load in a fibre at the point of fracture (refer to 3.3.5 for details of the definition). The value of r is determined by the mechanism of load transfer from fibre

to fibre in a sheet. The literature review (Chapter 2) shows that the shear lag model has been the most commonly used theory for load transfer in paper.

According to the shear lag theory, the load distribution along a fibre can be expressed as (Räisänen 1997):

$$\sigma_f(x,k) = E\varepsilon_x\left(1-\frac{\cosh kx}{\cosh(kl_f/2)}\right) \qquad \textbf{8. 4}$$

where E is the elastic modulus of the sheet, ε_x is the strain of the sheet in the direction of the fibre, l_f is the fibre length and k is an adjustable parameter, the value of which is determined by the assumed stress transfer mechanism.

The average load in the fibre can be calculated by integrating Equation 8.4. The value of r is then calculated by:

$$\frac{1}{r} = \left[1-\frac{2\tanh kl_f/2}{kl_f}\right] \qquad \textbf{8. 5}$$

The shear lag model for the network elastic modulus, E_n, is given by (Räisänen 1997; Räisänen, Heyden et al. 1997):

$$E_n = \frac{3qD_w^2E_f}{8}\left[1-2\frac{\tanh kl_f/2}{kl_f}\right] \qquad \textbf{8. 6}$$

In the high density limit, the shear lag model for a 2-D network is also written as:

$$E_n = \frac{3}{8}E_f D_w^2\left[q-Kq_c\right] \qquad \textbf{8. 7}$$

Here $q_c = 5.71/l_f$ is the percolation density (the smallest number of fibres per unit area for forming a fibre network (Pike 1974) and D_w is fibre width. In a 2-D network, the density, q, is defined as the total fibre length per unit area, whereas in a 3-D network (real paper), of course, density is given by the total mass per unit volume. The correspondence between the two densities is best established through the number of bonds per fibre. This was approximately given by $q/q_c \approx \pi l_f/11.42l_s$, in which $l_s = 1/N_c$ is the average length of free fibre segments (Corte 1962; Pike 1974) and N_c

has been previously defined by us as the number of bonds per unit fibre length. Thus q and N_c are related by:

$$q \approx \pi l_f q_c N_c / 11.42 \qquad \textbf{8. 8}$$

Comparing Equation 8.6 with Equation 8.7 and substituting N_c for q by using Equation 8.8, we can get:

$$k = \frac{\pi}{5.71}\frac{N_c}{K} \qquad \textbf{8. 9}$$

Bringing Equation 8.9 into Equation 8.5 then yields:

$$\frac{1}{r} = 1 - \frac{K}{0.275 N_c l_f} \qquad \textbf{8. 10}$$

The question for determination of the value of r becomes the determination of the value of K, which is referred to as the coefficient of load transfer in the literature (Aström, Saarinen et al. 1994; Räisänen 1997), and the number of fibre-fibre contacts per unit length of fibre, N_c, in the sheet. In Chapter 3 we have presented a model for number of fibre-fibre contacts in paper and the model has been fully verified in Chapter 7. Here we calculate N_c by using the model for number of fibre-fibre contacts. The value of K can be determined by different types of shear lag analysis. In the following subsections, we will discuss different types of shear lag analysis for determining the value of K and then r.

8.3.1 Determination of r by fitting elastic modulus data to shear lag model

Substituting Equation 8.8 into Equation 8.7 and rearranging yields the following expression:

$$\frac{8}{3}\frac{E_n l_f}{5.71 D_w^2 E_f} = 0.275 N_c l_f - K \qquad \textbf{8. 11}$$

We then plot $E_n l_f / D_w^2 E_f$ against $0.275 N_c l_f$. As shown in Figure 8-3, a very good linear relationship is found for each sample group. The same linear relationship has been found from simulations by Aström et al (Aström, Saarinen et al. 1994) and Räisänen et al (Räisänen 1997). Linear extrapolation from high densities down to

$E_n = 0$ gives $K = 1.82$ for cut fibres, $K = 4.29$ for the rejects and $K = 4.80$ for the accepts. These values are very close to those obtained by simulations in the work of Räisänen et al and Aström et al (Aström, Saarinen et al. 1994). Räisänen et al reported that the value of K was in the range of 3.5 to 4.3 for networks with flexible bonds. For networks with rigid bonds, Aström et al found K was in the range of 2.1 to 2.8.

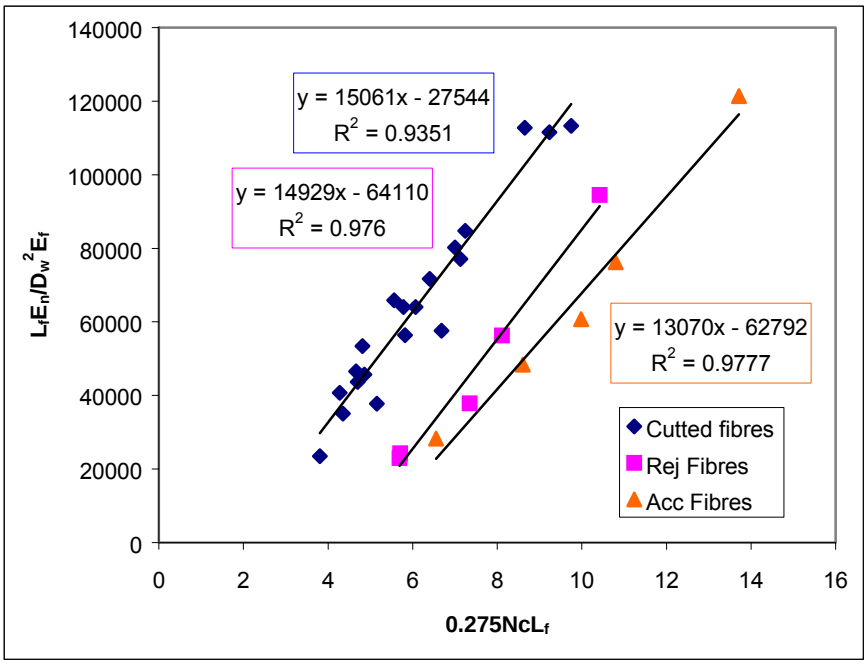

Figure 8-3 Plot between $E_n l_f / D_w^2 E_f$ and $0.275 N_c l_f$

The values of K for the cut fibres, accepts and rejects were then brought into Equation 8.9 to calculate values of r for these samples. The calculated values of r are plotted in Figure 8-4 against sheet density for the accepts, rejects and cut fibres. It can be seen from the figure that the calculated values of r slowly decrease with sheet density. The values of r range from 4.1 for the lowest density sheets to 1.2 for the denser sheets. These values of r were then used to calculate the tensile strength with Equation 8.3. Figure 8-5 compares the calculated tensile index with the measured tensile strength for these samples.

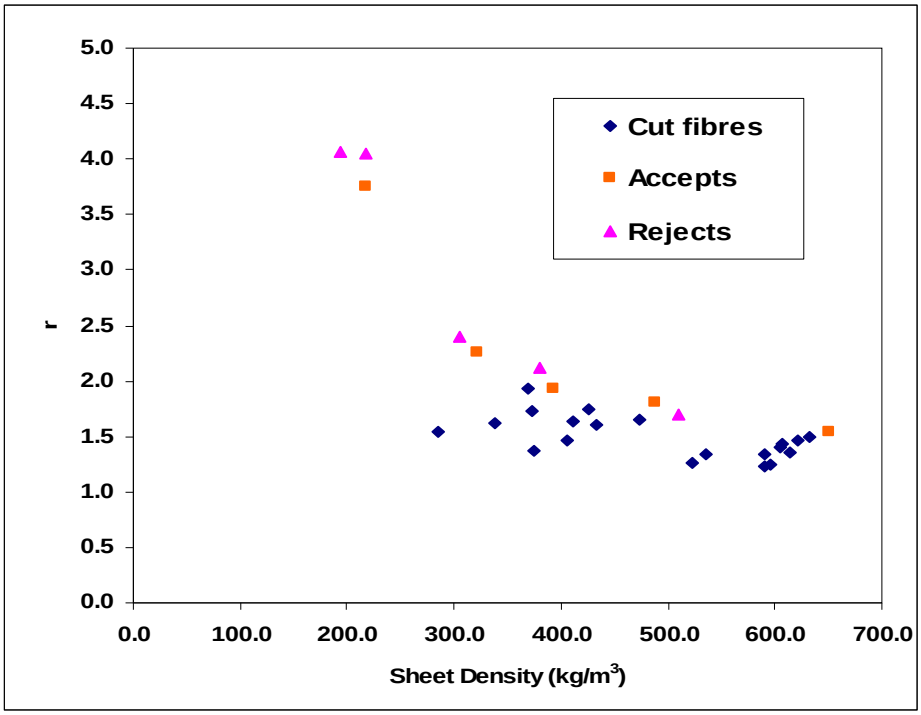

Figure 8-4 Relationship between sheet density and the value of r determined from elastic modulus data

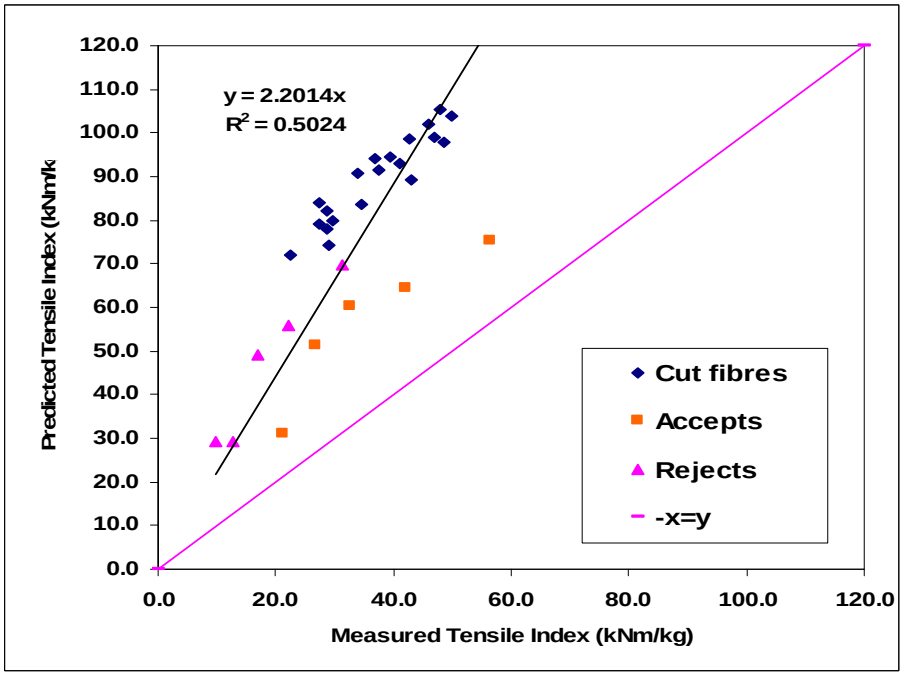

Figure 8-5 Comparison between the measured and predicted tensile index by the fibre fracture model, with r determined from the elastic modulus data.

As can be seen in Figure 8-5, there is a reasonable correlation between measured and predicted tensile index with an R^2 of 0.5. However, the slope of the correlation is 2.2, indicating either that the simple fibre fracture model for paper strength is not correct or

that the shear-lag formulation for the elastic properties does not apply to the fracture of paper.

8.3.2 Determination of r by Räisänen et al shear lag analysis

(Räisänen 1997) et al extended Cox's shear lag model to flexible bonds. From their work, K is given by:

$$K = \frac{\pi}{5.71}\sqrt{1+\nu+R_f\frac{11.4}{\pi}\frac{q}{q_c}} \qquad \textbf{8. 12}$$

where $R_f = (l_b E_f D_w^2 / l_f E_b D_b^2)$ is the ratio of the spring constants of the whole fibre and the bond. The spring constants are defined as $k_i = E_i D_i^2 / l_i$ ($l_i = length$, $E_i = modulus$ and $D_i = width$, $i = w,b$ for fibres and bonds, respectively). Substituting $q/q_c \approx \pi l_f / 11.4 l_s$ and $l_s = 1/N_c$ into equation 8.9, produces:

$$K = \frac{\pi}{5.71}\sqrt{1+\nu+R_f N_c l_f} \qquad \textbf{8. 13}$$

Bringing Equation 8.12 into Equation 8.9, and then into the fibre fracture model for tensile strength (Equation 8.3), we get:

$$T = \frac{8}{9}\left[1-\frac{2\tanh\dfrac{N_c l_f}{2\sqrt{1+\nu+R_f N_c l_f}}}{\dfrac{N_c l_f}{\sqrt{1+\nu+R_f N_c l_f}}}\right] * T_z \qquad \textbf{8. 14}$$

This is the final form of the model for tensile strength if the value of r is determined by Räisänen et al shear lag analysis. In Equation 8.13, R_f is determined by the rigidity of the bonds in the sheet. For the rigid bond case, $R_f \to 0$. Very flexible bonds give a large value for R_f. As mentioned before, $R_f = (l_b E_f D_w^2 / l_f E_b D_b^2)$. There is no way to measure the bond length l_b. In the simulation work by Räisänen et al (Räisänen, Heyden et al. 1997), a bonding element was inserted with a fixed length of

$l_b = 5 \times 10^{-5} l_f$ and width $D_w = D_f$. In this way it was determined that $R_f = 5 \times 10^{-5}$ for rigid bonds and $R_f = 5 \times 10^{-3}$ for flexible bonds.

For this work, we treated R_f as an adjustable parameter. The value of R_f was determined by optimising the fit of the measured tensile index with the calculated tensile index by Equation 8.14. The best fit result is shown in Figure 8-6 and the corresponding r values are shown in Figure 8-7. As can be seen in Figure 8-6, the predictions do not fit the measurements well. The optimised value of R_f was 5.1, which is far greater than that in the simulations by Räisänen et al (Räisänen, Heyden et al. 1997). This large value of R_f implies that the bonds in the network are so flexible that they will not break under any strain, which is physically unreasonable. It appears that the shear lag analysis by Räisänen et al cannot calculate correctly the value of r. Similar to the tensile strength, the correlation between sheet density and the value r is also poor (Figure 8-7).

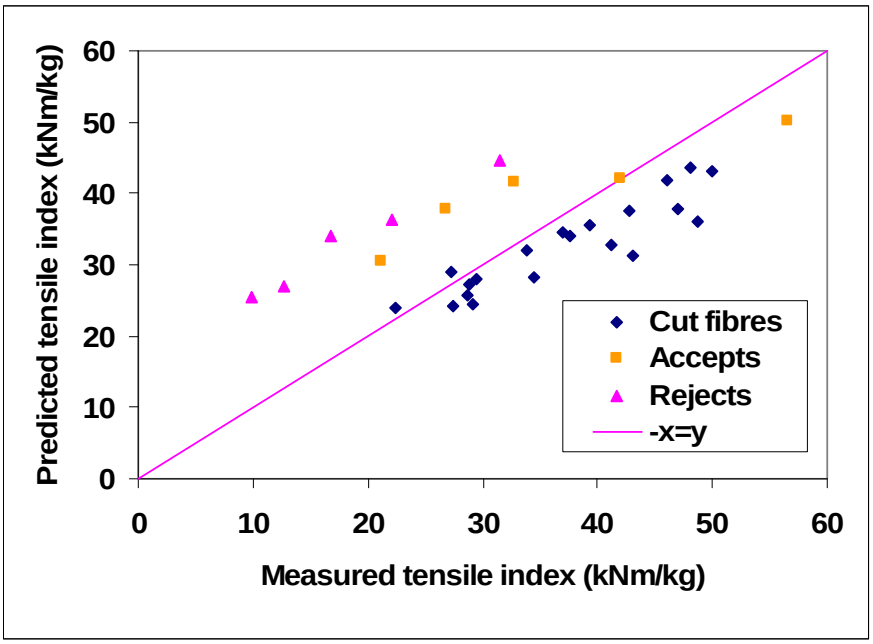

Figure 8-6 Comparison between the measured and the predicted tensile index by the fibre fracture model. r determined from Räisänen et al. shear lag analysis.

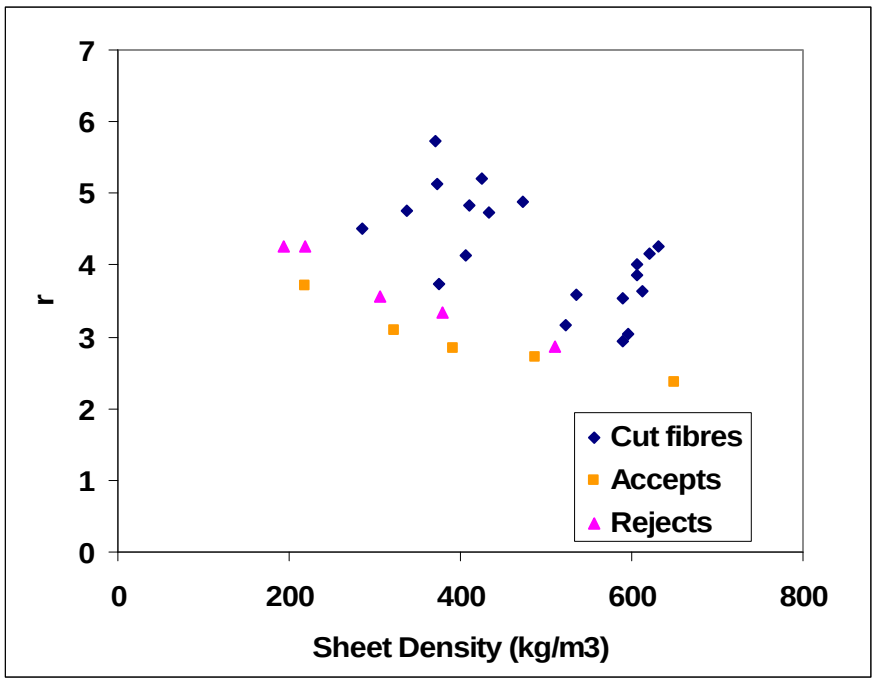

Figure 8-7 The plot of sheet density against the value of r determined from Räisänen et al shear lag analysis

8.3.3 Determination of r by Aström et al shear lag analysis

Aström et al (Aström, Saarinen et al. 1994) presented the following ad hoc relationship from summarising their simulations:

$$k \approx (a + bD_w / l_f) * q / q_c \qquad \textbf{8. 15}$$

Where a and b are constants. This expression can also be written as:

$$k \approx \frac{\pi}{11.42} * \frac{l_f}{l_s} * (a + bD_w / l_f) = \frac{\pi}{11.42} * N_c l_f * (a + bD_w / l_f) \qquad \textbf{8. 16}$$

This shows that the value of k is determined by the number of fibre-fibre contacts per fibre and the aspect ratio of the fibre. Bringing Equation 8.15 into Equation 8.8, and then into the model for tensile strength (Equation 8.3), we get the final form of the model for tensile strength with the Aström shear lag analysis as:

$$T = \frac{8}{9} * \left[1 - \frac{2 \tanh \frac{\pi}{11.42} * N_c l_f * (a + bD_w / l_f) / 2}{\frac{\pi}{11.42} * N_c l_f * (a + bD_w / l_f)} \right] * T_z \qquad \textbf{8. 17}$$

We allowed *a*, and *b* to be adjustable parameters and varied them to find the best fit between the predicted tensile index and the measured tensile index. For the best fit, $a = 0.08$ and $b = 11.2$. This corresponds $K = 11.7$, which is much higher than that obtained from the elastic modulus data and the values from literature (Aström, Saarinen et al. 1994; Räisänen, Heyden et al. 1997).

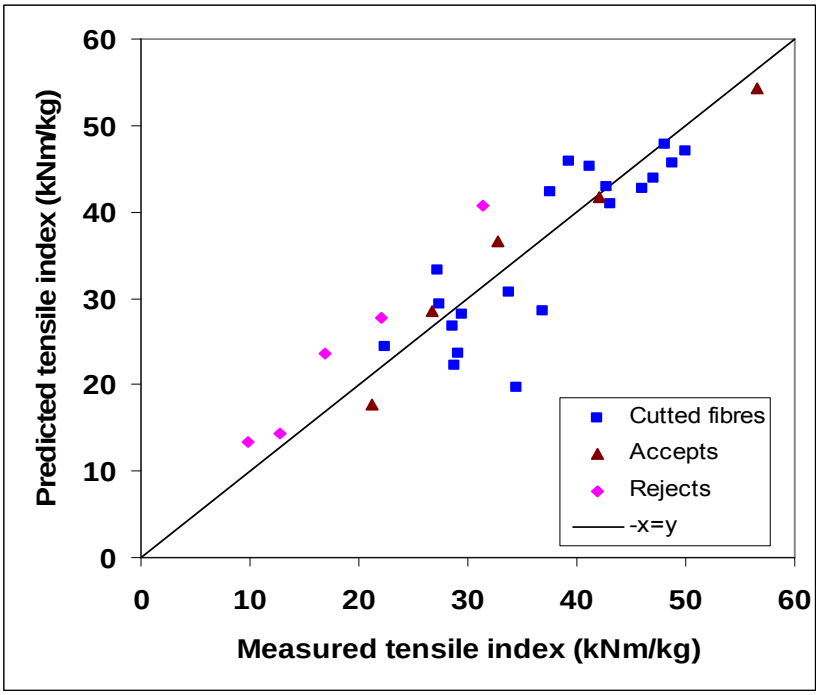

Figure 8-8 Comparison between the measured and the predicted tensile index by Equation 8.17. *r* was determined from Aström et al. shear lag analysis.

As shown in Figure 8-8, the data points lie much closer to the x-y line compared to that obtained by Räisänen et al shear lag analysis. The measurements and the predictions have a correlation coefficient of $R^2 = 0.79$ and a slope = 0.96. Also a good correlation was seen between the sheet density and the value of r determined from Aström et al shear lag analysis for the different samples (see Figure 8-9). The good correlation does not necessarily mean that the Aström et al shear lag analysis provides a physically reasonable value of r. It is not surprising that a good correlation can be generated as two fitting parameters are available in Equation 8.16.

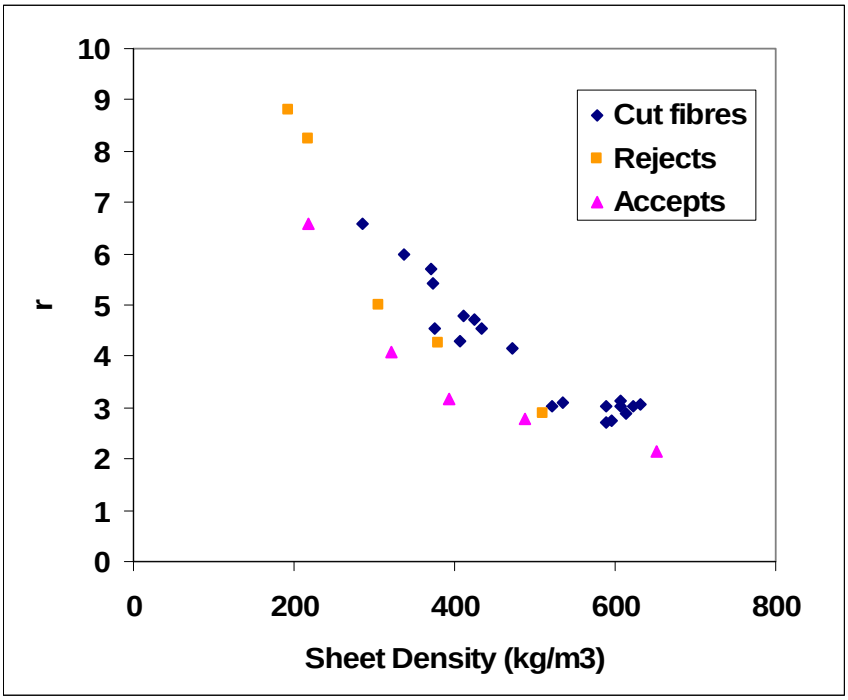

Figure 8-9 The plot of sheet density against value of r determined from Aström et al. shear lag analysis

The high value of K produced from this fit, in comparison to the much lower values obtained from fitting the elastic modulus data (refer to Figure 8-3) has the physical meaning that the stress transfer in the fibre was much less efficient at fracture than it was under elastic loading. The most reasonable explanation for this is bond failure within the samples before fracture starts. This has been experimentally observed in the literature (Niskanen, Alava et al. 1999). Bond failure will decrease the number of crossings of which a fibre can be loaded and thus increase the distance from the fibre end required to obtain the maximum load. However, such bond failure decreases the validity of shear-lag model itself, as the model assumes that stress transfer into the fibre is controlled by one parameter, k, which is uniform along the length of the fibre. Obviously some means of analytically accounting for fibre bond breakage is required. An initial attempt doing this is described in the next section.

8.4 Direct load transfer theory

8.4.1 The theory and network model

Räisänen et al (Räisänen, Heyden et al. 1997) believed that most stress-transfer along a fibre is by direct axial transfer of stress. However, no explicit expression or any kind of mathematical method was given for calculating the stress-transfer. Batchelor has recently developed a method for calculating stress-transfer based on the direct load transfer theory (see Appendix E). The main achievement of this theory is that it allows for the stress transfer to vary from point to point. Thus distributions in the properties of the crossing fibres can be modelled as well as different modes of stress transfer. The theory applies for linear transfer between the local displacement of the fibre and the displacement of the surrounding matrix. The theory assumes the fibre and fibre network to be purely elastic. The theory is based on a different type of approach where all displacements at contacts can be expressed in terms of the next displacement at the next contact along.

Figure 8-10 shows half the fibre of interest and crossing fibres. Each of the crossing fibres is then attached to the paper network. If the network is strained, then force will be transmitted into the fibre of interest from the crossing fibres. If the force delivered at the j^{th} contact is F_j, then assuming the fibres are linear elastic, it can be shown that the displacement from straining the first segment from the fibre mid-point is (see Appendix E for detailed derivation):

$$\delta_1 = \frac{1}{EA} x_1 \sum_{j=1}^{j=i} F_j - \varepsilon x_1 \qquad \textbf{8. 18}$$

where E and A are the elastic modulus and cross-sectional area, respectively, of the fibre.

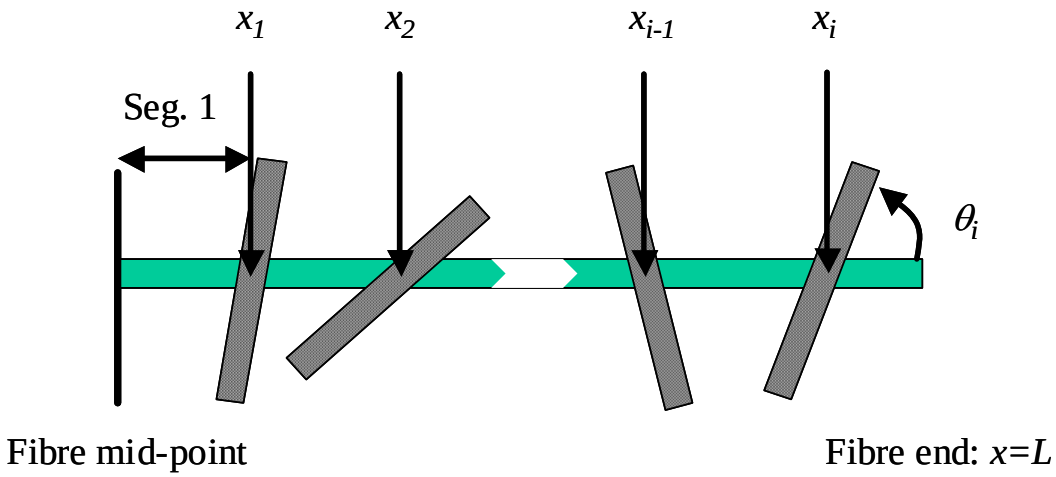

Figure 8-10 Unstrained half fibre of length, L, with i crossing fibres

The displacement at the second contact is

$$\delta_2 = \frac{1}{EA}\left(x_1 \sum_{j=1}^{j=i} F_j + (x_2 - x_1) \sum_{j=2}^{j=i} F_j \right) - \varepsilon x_1 - \varepsilon (x_2 - x_1) \qquad \textbf{8. 19}$$

which simplifies to

$$\delta_2 = \frac{1}{EA}\left(x_1 F_1 + x_2 \sum_{j=2}^{j=i} F_j \right) - \varepsilon x_2 \qquad \textbf{8. 20}$$

Extending this process it can be shown that for n^{th} and $n-1^{\text{th}}$ contacts that

$$\delta_n = \frac{1}{EA}\left(\sum_{j=1}^{j=n-1} x_j F_j + x_n \sum_{j=n}^{j=i} F_j \right) - \varepsilon x_n \qquad \textbf{8. 21}$$

$$\delta_{n-1} = \frac{1}{EA}\left(\sum_{j=1}^{j=n-2} x_j F_j + x_n \sum_{j=n-1}^{j=i} F_j \right) - \varepsilon x_{n-1} \qquad \textbf{8. 22}$$

and Equation 5 can be rewritten as

$$\delta_{n-1} = \delta_n + (x_n - x_{n-1}) \left(\varepsilon - \frac{1}{EA} \sum_{j=n}^{j=i} F_j \right) \qquad \textbf{8. 23}$$

Thus the displacement at each contact can be expressed in terms of the forces (which in turn are a function of the displacements) developed at all the contacts further along the fibre towards the end as well as the displacement of the next contact along the fibre.

Thus δ_{i-1} can be written in terms of δ_i; δ_{i-2} can be written in terms of δ_{i-1} and thus in terms of δ_i, and a similar chain can be developed such that each of the displacement can be expressed in terms of δ_i, the displacement at the final crossing nearest the fibre end. The displacements at all the fibre crossings can be expressed in terms of δ_i and as δ_i is given by

$$\delta_i = \frac{1}{EA}\left(\sum_{j=1}^{j=i} x_j F_j\right) - \varepsilon x_i \qquad \textbf{8. 24}$$

It is possible to solve this equation to determine δ_i and thus to uniquely determine the displacements at all crossings, provided that F can be expressed as a function of displacement.

The model assumes that stress transfer takes place directly from direct transfer of axial loads in the crossing fibres and that the crossing fibre has a distance, l_c, before it is rigidly bonded into the surrounding network or matrix. Figure 8-11 shows such a single fibre contact, before and after the matrix is strained. For this analysis, the reference point, $x = 0$, is set at the position of the crossing point in the unstrained system. We need to note that for the rest of the analysis $x = 0$ corresponds to the mid-point of the fibre.

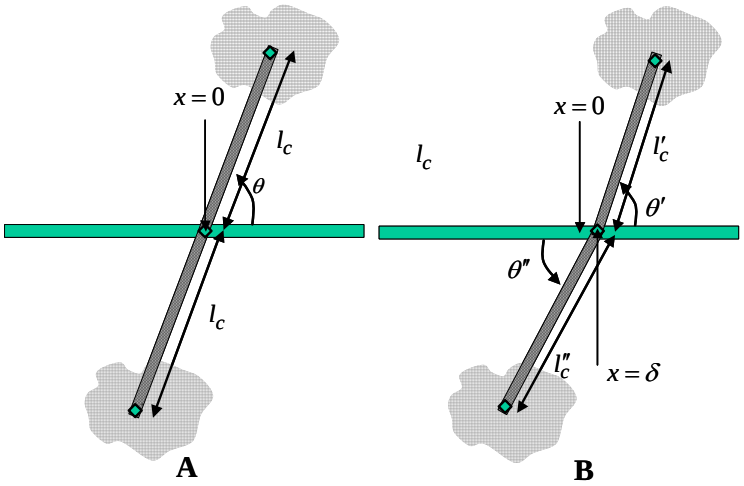

Figure 8-11 Part A: A crossing fibre, with a crossing angle of θ and a distance of l_c until it is firmly bonded into the surrounding matrix. The point at which the fibre crosses is $x = 0$. Part B: The same fibre crossing after the matrix has been strained by ε and the crossing point has also moved a distance of δ from $x = 0$.

By using the above fibre-fibre contact model, it has been shown that F can be expressed as:

$$F = -2E_c A_c \cos^2(\theta)\delta / l_c \qquad \textbf{8. 25}$$

where E_c and A_c are the modulus and cross-sectional area of the crossing fibre, respectively and θ is the crossing angle.

It should be noted that the result, that the force is linearly proportional to the displacement of the contact relative to the applied strain, is the same assumption made in the shear-lag model. The force function, Equation 8.25, is for direct load transfer only and ignores the effect of shear in fibre (see Appendix E for details)

Before doing any calculation of load distribution, a model for a fibre connected with the fibre network, as shown in Figure 8-10, has to be constructed first. As discussed in Chapter 7, the free fibre length has a Weibull distribution as given by Equation 7.1. The cumulative density function for Equation 7.1 is:

$$F(g) = 1 - e^{-(g/b)^c} \qquad \textbf{8. 26}$$

where b is the scale parameter, and c is the shape parameter for the Weibull density function, and $b, c > 0$, and $g \geq 0$ is the free fibre segment length. $F(g)$ ranges from 0 to 1. The values of b and c for some samples in this project have been determined experimentally, as presented in subsection 7.3.2.

Rearranging Equation 8.26, the free fibre segment length can be given as:

$$g = b\left[\left(-\ln(1 - F(g))\right)^{\frac{1}{c}}\right] \qquad \textbf{8. 27}$$

Equation 8.27, in which $F(g)$ is a random number between 0 and 1, can be used to generate the free fibre length.

Similarly, in a random sheet, the angles of the fibres crossing the fibre of interest can be calculated by the follow equation:

$$\theta = \arcsin\left(F(\theta)\right) \qquad \textbf{8. 28}$$

where $F(\theta)$ is a random number between 0 and 1.

The crossings for the fibre of interest were then constructed using the following scheme. As the method itself only considers the strain from the middle of the fibre ($x = 0$), this was taken as the start point. The position of the first crossing fibre was then calculated by generating a random number for F, calculating g using Equation 8.28 and dividing this by half for the first contact only. The next fibre crossing position was generated by calculating the next free fibre length and then adding this to the first position. This process was repeated until the end of the fibre is reached. A crossing angle was generated for each of the crossing fibres by using Equation 8.29.

The above calculations were conducted by using a programme written in Matlab software (see Appendix D for details). We assumed that no fibres were broken and did not consider the non-uniformity of the paper.

8.4.2 Simulations without bond breakage

The simulations show that if we do not allow bond breakage, the value of r is independent of external strain and is a constant for a given fibre. The calculated r values are plotted against the sheet density in Figure 8-12 showing a weak negative correlation. The r values for no bonds failure were brought into the fibre fracture model (Equation 8.3) to calculate the tensile index for samples of the cut fibres, the accepts and rejects and the results are compared with the corresponding measurements in Figure 8-13. Each point in Figure 8-13 is an average of ten simulations. Clearly, the calculations significantly overestimate the tensile index. This suggests the existence of bond breakage before fracture of the paper and its strong influence on the value of r.

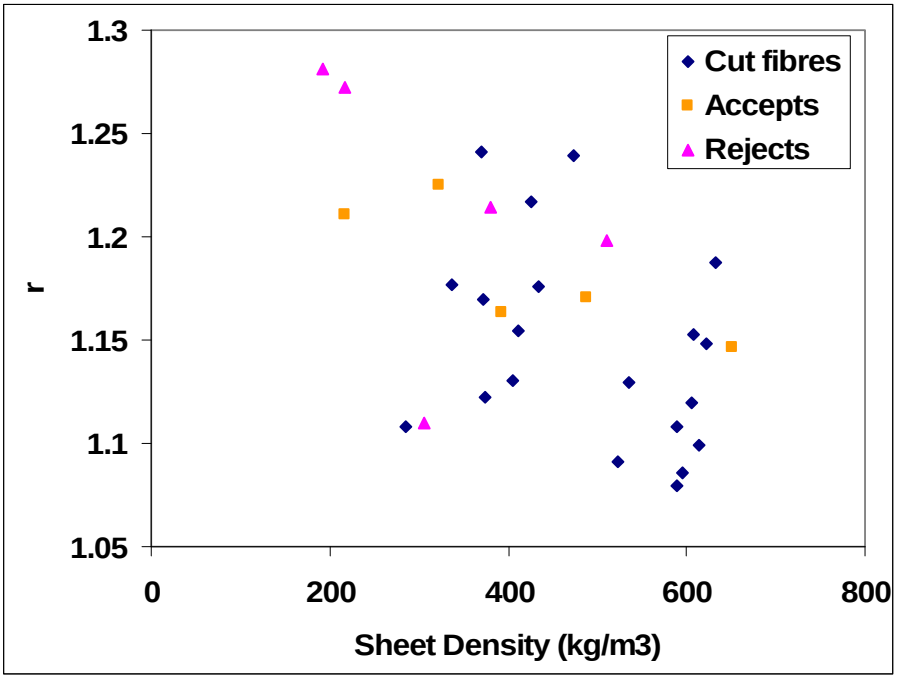

Figure 8-12 The plot of sheet density against value determined by simulations allowing no bonds breakage.

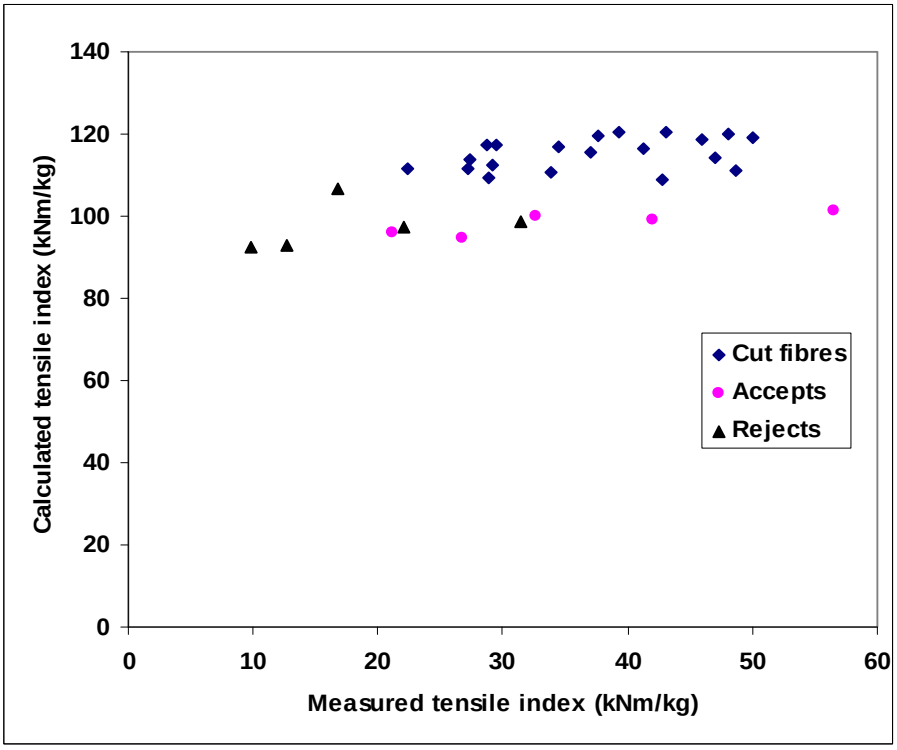

Figure 8-13 Comparison between measured tensile index and calculated tensile index by the fibre fracture model where r is determined by simulations allowing no bonds break.

8.4.3 Summary of values of r calculated by different methods

The values of r calculated from the above different methods are summarised in Table 8-1. Clearly, the r values significantly differ from method to method. As discussed above, the r values calculated by Aström et al shear-lag analysis with two fitting parameters gave the best correlation between the measured tensile strength and the predicted tensile strength. The good correlation do not necessarily mean that the Aström et al shear-lag analysis is better than the others. However, it is probably true that the r values of the samples used here are in the range of 2.1 to 8.8, which is the prediction by Aström et al shear-lag analysis.

Table 8-1 Summary of values of r calculated by different methods

Sample	Aström Shear lag analysis	Räisänen Shear lag analysis	Elastic Modulus Fitting	Simulation (no bond breakage)
L_0P_1	6.6	4.5	1.5	1.1
L_0P_2	4.6	3.7	1.4	1.1
L_0P_3	3.0	3.2	1.3	1.1
L_0P_4	2.7	2.9	1.2	1.1
L_0P_5	2.8	3.0	1.2	1.1
L_1P_1	6.0	4.8	1.6	1.2
L_1P_2	4.3	4.1	1.5	1.1
L_1P_3	3.1	3.6	1.3	1.1
L_1P_4	3.0	3.5	1.3	1.1
L_1P_5	2.9	3.6	1.4	1.1
L_2P_1	5.4	5.1	1.7	1.2
L_2P_2	4.8	4.8	1.6	1.2
L_2P_3	4.6	4.7	1.6	1.2
L_2P_4	3.0	3.9	1.4	1.1
L_2P_5	3.1	4.0	1.4	1.2
L_3P_1	5.7	5.7	1.9	1.2
L_3P_2	4.7	5.2	1.7	1.2
L_3P_3	4.2	4.9	1.6	1.2
L_3P_4	3.0	4.2	1.5	1.1
L_3P_5	3.1	4.3	1.5	1.2
AcP_1	8.8	3.7	3.8	1.2
AcP_2	8.3	3.1	2.3	1.2
AcP_3	5.0	2.8	1.9	1.2
AcP_4	4.3	2.7	1.8	1.2
AcP_5	2.9	2.4	1.5	1.1
$RejP_1$	6.6	4.3	4.1	1.3
$RejP_2$	4.1	4.3	4.0	1.3
$RejP_3$	3.2	3.6	2.4	1.1
$RejP_4$	2.8	3.3	2.1	1.2
$RejP_5$	2.1	2.9	1.7	1.2

8.4.4 Simulations with bond breakage

In the following simulations, we included bonds failure. The loads in the bonds were calculated and compared with the strength of the bonds. The bond was broken and removed from the fibre of interest if the load in the bond was greater than the strength of the bond. The bond strength was estimated to be 3000kN/m^2 according to the prediction made by Page equation (refer to subsection 8.2).

Figure 8-14 shows an example of load distribution in a half fibre. This is one simulation for sample SL0. As can be seen in Figure 8-14, the load in the fibre increases as the external strain is increased from 0.001 to 0.003. Over this range no bonds have failed and the load distribution scales directly with strain. The first bonds failed in the simulation when the external strain was increased to 0.004. Successive simulations are shown for this strain. This is because the simulation proceeds in an iterative manner. Whenever bond fracture occurs the stress distribution in the fibre is then recalculated and the loads in the bonds rechecked against bond strength. Frequently it is found that the redistribution in the load has caused bond failure in the nearby bonds. Bond failure tends to start at the ends of the fibres and move inwards. This can be observed in the simulation shown in Figure 8-14, where the data set with the solid squares represents the last simulation. Interestingly, it can be seen that while the maximum load in the fibre changes very little, the average load across the fibre has dropped sharply. These results dramatically increase the r value. The simulations showed that the r value is a 'dynamic value' which was significantly affected by the bond breakage. For the simulation in Figure 8-14, the r value gradually increased from 1.1 to 3.0 as the number of bonds broken was increased by increasing the external strain. Although the values of r can be calculated during the whole process, these values cannot be applied to our simple fibre fracture model because no fibre breakage occurs during the process.

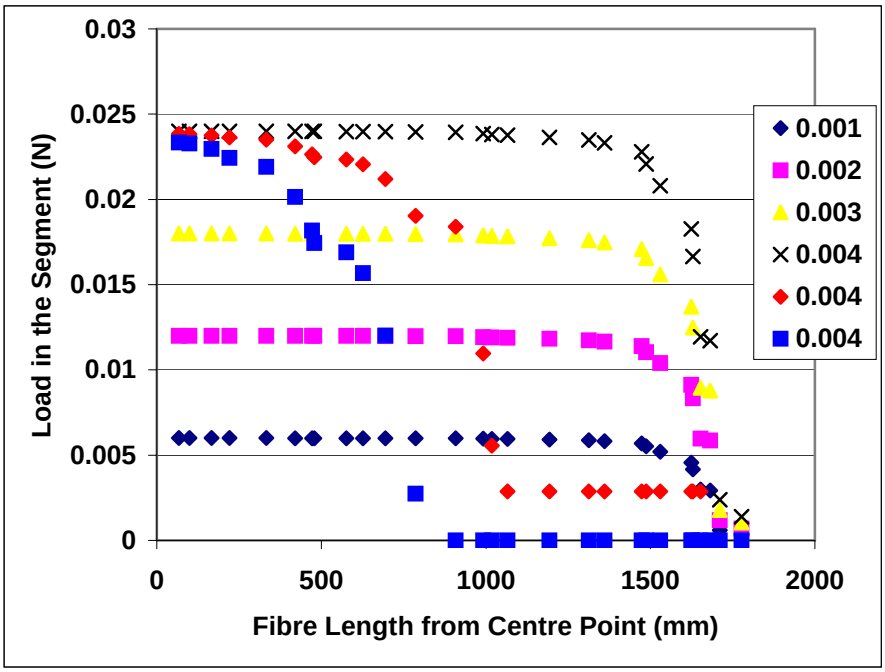

Figure 8-14 Load distribution in a fibre of interest as the global strain is increased

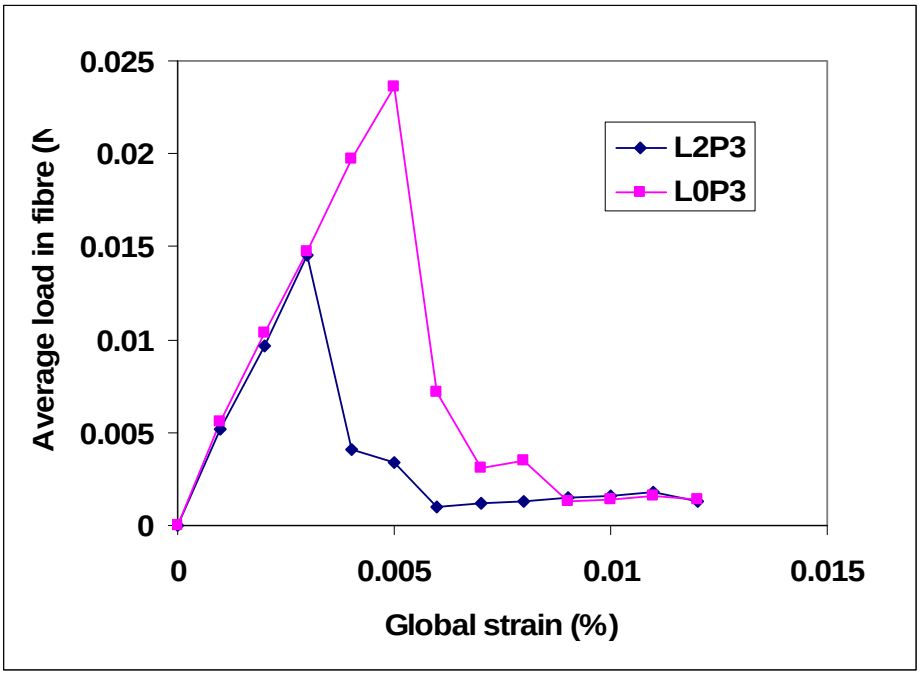

Figure 8-15 The relationship between the global strain and the average load in the fibre of interest.

Interestingly, when the average load was plotted against the global strain, it was found that the average load in the fibre increases to a peak point and then drops abruptly as the

global strain is increased (see Figure 8-15). We then define the average load in the fibre just before the abrupt drop of the load in the fibre as the peak average load. This peak average load represents the maximum load holding the fibre under the simulation conditions. It is assumed that the abrupt drop of average load corresponds to the breakage of the sheet. The peak average load was then used to calculate the tensile strength of the sheet. The calculation is shown as follows.

The number of fibres per unit width of the sheet can be written as:

$$n_f = \frac{\cos\theta * G}{A_{ap} * \rho} \qquad \textbf{8. 29}$$

where θ is the overall angle a fibre made to the cross-section of the sheet, G is grammage, A_{ap} is the apparent fibre wall area, which is the wall area cut in the cross-section, ρ is the density of the fibre wall.

The tensile strength of the sheet breaks as the average load in the fibre reaches the peak can be calculated by:

$$T_b = \frac{3}{8} * \frac{n_f * F_{ave}}{G} \qquad \textbf{8. 30}$$

where F_{ave} is the peak average load in the fibre as indicated in Figure 8-15 and 3/8 is the constant which applies for a randomly oriented sheet.

Table 8-2 Calculated tensile index by using peak average load from simulations with bond breakage summarises the calculated tensile index by using the peak average load from simulations with bond breakage.

Table 8-2 Calculated tensile index by using peak average load from simulations with bond breakage

	Apparent Fibre Wall Area (μm^2)	Grammage (g/m^2)	N0.of fibre (no. per unit sheet width)	F_{ave} (N)	Calculated Tensile Index (kNm/kg)	Measured Tensile Index (kNm/kg)
L_0P_1	235	66	156734	0.015	13.11	34.45
L_0P_2	229	65	158318	0.019	17.91	36.98
L_0P_3	223	64	161618	0.024	23.15	45.98
L_0P_4	228	64	156845	0.020	18.13	48.04
L_0P_5	233	64	154345	0.026	23.43	49.95
L_1P_1	247	65	147380	0.012	9.88	29.11
L_1P_2	221	65	166354	0.015	14.63	28.70
L_1P_3	236	64	152057	0.011	10.25	29.52
L_1P_4	238	64	151251	0.021	18.73	37.63
L_1P_5	236	63	150401	0.022	19.99	43.11
L_2P_1	226	64	158940	0.018	16.31	28.82
L_2P_2	230	66	161809	0.017	15.15	33.78
L_2P_3	234	66	157754	0.023	21.00	42.82
L_2P_4	233	66	157846	0.022	20.22	47.03
L_2P_5	232	65	158464	0.027	24.85	48.74
L_3P_1	226	65	161363	0.011	9.78	22.34
L_3P_2	230	66	160255	0.013	12.12	27.43
L_3P_3	234	66	157630	0.015	13.44	27.25
L_3P_4	233	65	157066	0.020	18.41	39.34
L_3P_5	232	65	157113	0.021	19.17	41.23
AcP_1	221	64	162936	0.008	7.84	21.17
AcP_2	224	68	169873	0.013	11.81	26.75
AcP_3	218	70	179809	0.016	15.85	32.70
AcP_4	231	72	174361	0.022	19.88	42.02
AcP_5	228	70	171332	0.027	25.07	56.52
$RejP_1$	259	62	135260	0.007	5.76	9.80
$RejP_2$	260	63	135744	0.006	4.94	12.77
$RejP_3$	270	68	141160	0.008	6.35	16.82
$RejP_4$	262	67	144192	0.013	10.64	22.06
$RejP_5$	254	69	152749	0.017	14.34	31.42

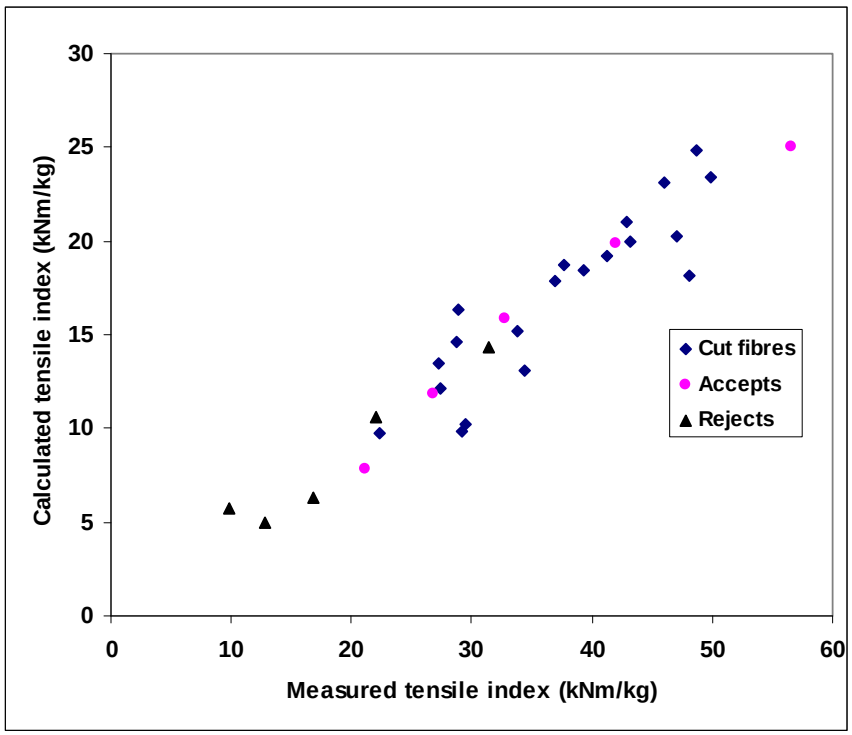

Figure 8-16 Comparison between measured tensile index and predicted tensile index by the peak average load.

Figure 8-16 compares the predicted tensile indices with the measurements. Each of the points is the average of ten simulations. It shows a very good correlation between the calculations and the measurements, and all the data points for the different series seem to fall on the same straight line. However, the calculations significantly underestimated the tensile index. The calculated strength is only about 1/3 of the measured strength. These results show that the bond break model significantly underestimates the tensile strength.

Not only do the simulations predict sheet strength of around 1/3 of the measured strength, but they also predict that the sheet will fail entirely through bond breakage. This is shown in Figure 8-17, which plots the estimated fibre strength calculated from the zero-span tensile strength against the peak load in the fibre. It can be seen that peak load in the fibre is always much less than the fibre strength.

The model provides an exact analytical solution to the stress-distribution along the fibre but depends for its accuracy on the expressions for the stress-transfer into the fibre from the surrounding matrix. These are clearly under-estimating the load transfer.

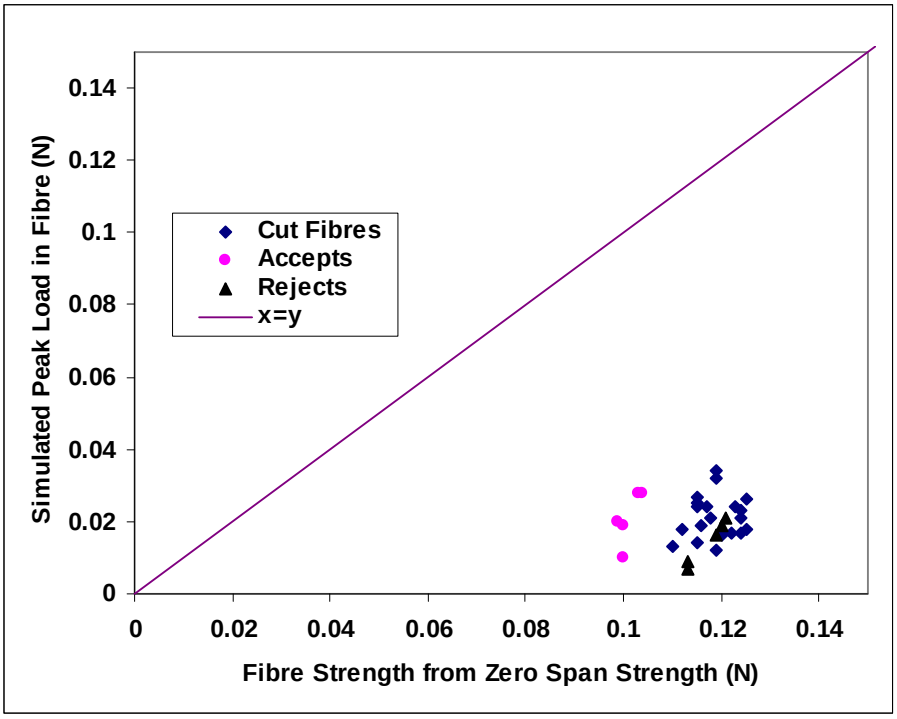

Figure 8-17 Fibre strength calculated from zero span strength against simulated peak load in the fibre

The previous discussion has shown that the fibre fracture model without bond breakage significantly overestimated tensile strength. The bond break model presented here significantly underestimates the tensile strength. It appears that to successfully predict the fracture of paper, the bond breakage model will need to be modified to increase maximum loads and strain at break. The following factors will need to be considered:

- Allowing fibres crossing at 90^{o} to contribute to load transfer via shear mechanism. The major difficulty here is how to treat the shear contribution of fibres not crossing at 90^{o}.
- Allowing crossing fibres at broken bonds to continue to contribute force to fibre via a friction mechanism. In the current model, it is assumed that once a bond breaks then that crossing fibre is completely removed from the simulation. In reality, such fibres are likely to continue to transfer some load by fibre-fibre friction even after they have broken.
- Introducing plastic deformation into the fibre of interest. This will reduce the load at the fibre-fibre bonds for a given level of external strain.
- Including fibre fracture in the simulation.

The result will be a model in which bonds will break but at higher loads, allowing the fibre to be loaded until fracture. It is beyond the scope of this PhD to do this, but the data make it clear such a model combining both fibre and bond breakage is likely to deliver the model that we have sought.

8.5 Conclusions

The following conclusions are drawn from the work in this chapter:

- The Page equation can provide a reasonable prediction for paper strength only if the bond strength is used as a fitting parameter. The reason probably is that the Page equation is not correctly accounting for the effect that changes in fibre morphology has on paper strength.
- The value of r in the simple fibre fracture model of the tensile strength of paper has been determined by fitting elastic modulus data to shear lag model, by using Räisänen et al shear lag analysis and Aström et al shear lag analysis, respectively. The tensile strength of paper calculated by the simple fibre fracture model using the values of r determined by each of the shear lag analysis has been compared with the measured tensile strength of paper. Only when the r values determined by Aström et al shear lag analysis were used, did the predicted tensile strength showed a good correlation with the measured tensile strength. Given that two fitting were available parameters in the Aström et al shear lag analysis, the good correlation does not necessarily mean that the Aström et al shear lag analysis provides a physically reasonable value of r. The above findings suggest that the shear-lag formulation for the elastic properties does not apply to the fracture of paper.
- For the first time, an explicit expression of direct load transfer theory is available for calculation of the load distribution in a fibre in a strained network. It has been demonstrated that a model structure of a fibre connected to a fibre network can be constructed by using the two parameter Weibull density function. The load distribution in the model fibre has been simulated by using the direct load transfer theory. The simulations show that, when there is no bond breakage, the load distribution in the fibre shows a similar pattern to that predicted by the

shear-lag model and the peak load and the average load increase at the same rate as the global strain is increased. In other words, the value of r for a given fibre is independent of the external strain. When bond breakage is included, the simulations show that bonds start to break from the ends of the fibre as the external strain is increased. It has also been shown that the tensile strength calculated from the peak average load in the fibre has a very good correlation with the measured tensile strength although the predictions significantly underestimate the measurements. Further modifying the bond breakage model is likely to deliver the model for tensile strength that we have sought.

- Although great efforts have been made in this thesis to test the simple fibre fracture model for the tensile strength of paper, this has not been possible because none of the methods used can calculate the value of r in the model correctly. However, it has been shown in the bond breakage model (simulation) that the r value is a 'dynamic value', which is significantly affected by the breakage of bonds before the sheet breaks. Further modifying the bond breakage model by including fibre fracture is expected to provide better prediction of the sheet fracture and therefore better calculation of r value for testing the simple fibre fracture model. It is beyond the scope of this PhD to do this but will be done in the future work.